

Exploiting Object Symmetry for Efficient Grasping

Paper XXX

ABSTRACT

In this, paper we introduce an efficient representation for robot grasping that exploits symmetry properties of objects. The new representation forms a low-dimensional manifold, which can be used to identify the set of feasible grasps during a sequential manipulation task. We analyse the properties of this low-dimensional manifold and show that some of these properties can be used for fast manipulation planning. We apply the introduced representation and planner to bi-manual manipulation in humanoid robots.

1. INTRODUCTION

Robots with advanced dexterous capabilities have the potential to revolutionize important application domains such as healthcare, security, or manufacturing. Whether in structured environments such as factories, or unstructured environments such as homes, grasping is often the first step in the physical interaction between a robot and its surroundings. The generation of grasps on objects is therefore at the heart of plan generation for physical tasks. However, to date most grasp planning methods are mainly focused on generating physically stable grasps without incorporating immediate or future task constraints.

Many well established algorithms assume only a single action and do not include foresight and reasoning about next actions. However, when picking up a mug, it is important to select a grasp that facilitates the next action to be performed. For example, in case the next action is a pouring motion, the robot needs avoid grasps that would cover the rim of the object. In contrast, if any of the next actions involves placing the mug on the table, the robot cannot choose any grasp in which fingers touch the mug's base.

Many grasp representations are based on a floating hand, thereby representing only the end-effector and ignoring the embodiment of the entire robot in environment. As a result, infeasible grasps are generated and have to be pruned out in a post-processing step. This can be particularly limiting in bi-manual, sequential, and co-worker scenarios, in which the actions of one agent are likely to violate the constraints of another agent. In these scenarios, grasps need to be carefully chosen, such that they do not violate constraints imposed by a second arm, a human interaction partner, or a future

Appears in: *Proceedings of the 14th International Conference on Autonomous Agents and Multiagent Systems (AAMAS 2015)*, Bordini, Elkind, Weiss, Yolum (eds.), May, 4-8, 2015, Istanbul, Turkey.

Copyright © 2015, International Foundation for Autonomous Agents and Multiagent Systems (www.ifaamas.org). All rights reserved.

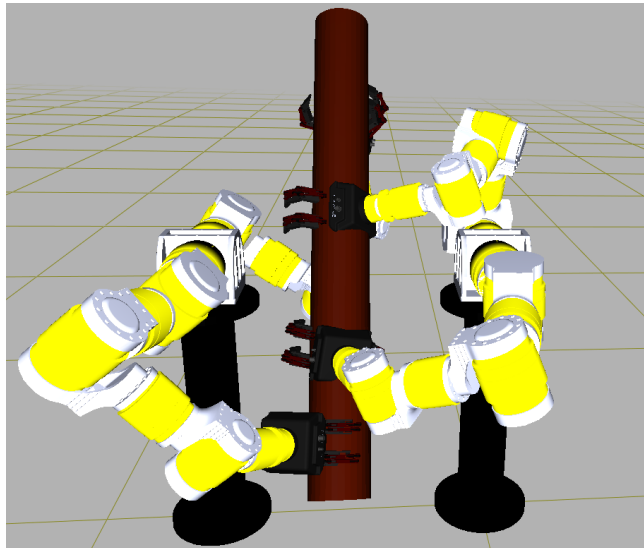


Figure 1: The manipulation of a heavy wooden log by two robots, planning for a pair of bimanual grasps

action.

In this paper, we address the issue of manipulation planning with task constraints. We are particularly interested in tasks that involve several subtasks or several interacting agents. Planning grasps for such tasks can rapidly become computationally infeasible due to the large search space. The key insight of this paper is that re-occurring patterns in the geometry of shapes can be exploited to drastically reduce the space of solutions. We will introduce a low-dimensional, object-centered representation for grasp planning which is based on rotational symmetries. The symmetric nature of the objects allows us to update our representation as the object is rotated around the axis of symmetry. *Since the object is symmetric any stable grasp can be rotated around the axis yielding a family of feasible grasps.* We will show that this basic property leads to a significant reduction of the search complexity in grasp planning. Specifically, this property allows us to generate multiple grasps around the object which is useful for bi-manual tasks and cooperative robot hand over tasks. Figure 1 demonstrates an example where a rotationally symmetric log is manipulated by two robots using both arms. In addition, it allows us to identify a single grasp that is useful for a sequence of tasks.

2. RELATED WORK

Robot grasping is a heavily studied sub-field of robotics. Until recently, most approaches have focused on the problem of generating stable grasps on objects. Given a model of an object, a hand shape is synthesized that allows the physically stable manipulation of the object [10, 11]. A prevalent approach is to modify the grasp parameters until a hand shape is found which is optimal w.r.t. a given criterion, such as force closure [15], or grasp wrench space [4]. For recent surveys of the grasp synthesis literature the reader is referred to [9] and [17].

To efficiently synthesize a variety of grasps, objects are often modelled using primitives, such as bounding boxes [8], medial axis representations [16], superquadrics [7], or simple geometrical shapes including cylinders, boxes and spheres [14]. Another way of increasing efficiency is by reducing the dimensionality of the space of possible hand configurations. In [5] and [2], dimensionality reduction techniques are used to project the space of hand shapes onto a low-dimensional manifold of two to three dimensions. However, in the above approaches, reachability and possible collisions during motion execution are only analyzed in a post-processing step after grasps are generated. Hence, possibly unreachable or unsafe grasp configurations are produced. Recent approaches have tried to bridge the divide through simultaneous grasp synthesis and motion planning [19]. Still, as noted in [6], looking solely at the stability of the grasp, or other immediate criteria ignores task constraints which are induced by the subsequent manipulations of the object. A grasp is often highly dependent on the task to be performed and should be chosen with next actions in mind.

Dang et al. [6] incorporate task constraints by semantically annotating grasps from a database. These grasps are then mapped onto a new object using local optimization. While this approach is a substantial step towards task-based grasp synthesis, it still requires prior human annotations of a grasp dataset. In a similar vein, Antanas et al. [1] use a probabilistic logic module to semantically reason about pre-grasp configurations with respect to the intended tasks. By exploiting symbolic world knowledge stored in object/task ontologies, they can infer appropriate grasps for a given task. A machine learning approach with a similar goal was introduced by Song et al. [18]. Their approach uses a Bayesian Network to learn task constraints for object manipulation.

The need for sufficient *foresight* during action selection has recently been discussed in the hierarchical planning literature [13]. Levihn and colleagues argue that look-ahead into future plans is important to avoid making short-sighted choices. While close in spirit to the work presented in our paper, the work of Levihn and colleagues concentrates on the task of moving among obstacles and does not include grasp synthesis.

In this paper, we show how inherent shape properties, specifically rotational symmetries, can be used to efficiently generate task-constrained grasps. Object symmetries have long been studied in the computer vision literature. Recently, various studies have indicated that symmetries can be exploited for grasping [12, 3]. However, these studies have mostly focused on how to generate complete meshes from partial point clouds.

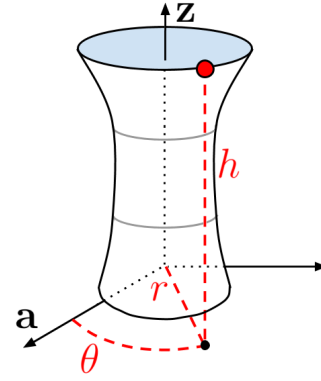


Figure 2: Cylindrical coordinate system to parameterize points on a rotationally symmetric object

3. MANIFOLD REPRESENTATIONS FOR ROTATIONALLY SYMMETRIC OBJECTS

Projecting manipulation constraints such as collisions with the environment and robot manipulator limitations (e.g. reachability) onto object surfaces can facilitate the search for feasible grasps. In this work, we demonstrate that particularly for rotationally symmetric objects, which do not have any surface protrusions or cavities, a number of grasping sub-problems such as finger placements, wrist pose, and collision-free inverse kinematics are simplified. Inspired by the texture mapping literature in computer graphics, we begin with the two-dimensional manifold representation of rotationally symmetric objects whose surfaces can be unwrapped into simple planes. The goal is to use this low-dimensional representation to accumulate multiple task constraints in the same local object space and then, efficiently identify grasps that satisfy all the future actions.

3.1 Cylindrical Surface Parametrization

Coordinate spaces characterized by rotations around an axis can be parametrized by cylindrical parameters where a vector \mathbf{z} represents the principal orientation and the polar axis \mathbf{a} captures the secondary direction in the reference plane perpendicular to \mathbf{z} . Using their intersection \mathbf{o} as the origin, any point in the Euclidean coordinate system can be represented in this coordinate system by computing the projection of the point onto the \mathbf{z} axis, its distance to the axis, and the angle between the polar axis \mathbf{a} and its projection onto the reference plane.

Figure 2 demonstrates the representation of a point on a rotationally symmetric object in terms of the parameters $[h, r, \theta]^T$ that correspond to the height along \mathbf{z} , the radius r of the circle parallel to the reference plane that includes the point, and the angle θ between \mathbf{a} and the point projection onto the reference plane. Note that the reference plane is arbitrarily placed on the bottom surface of the object and the polar axis can be freely chosen within this plane.

A significant observation about the representation of rotationally symmetric objects in cylindrical coordinates is the dependency between the radius r and the height h parameters. For a given shape S , all the points on S , at some height h along the principal axis \mathbf{z} , have the same distance r to the axis: $\forall \mathbf{p} \in S \text{ s.t. } \mathbf{p} \cdot \mathbf{z} = h, \text{ dist}(\mathbf{p}, \mathbf{z}) = r_S(h)$. The function

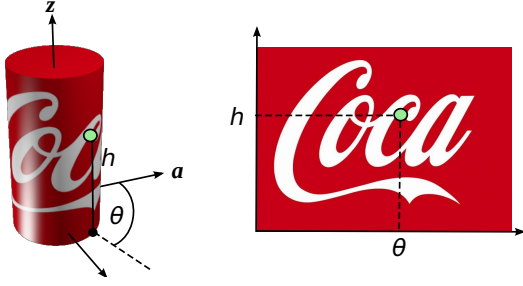


Figure 3: The points on the 3D surface (left) are projected onto a 2D cylindrical manifold.

$r_s(h)$ represents the inherent curvature of the shape - for instance, for a cylinder, $r = c$ for some constant c . Based on this observation, we can conclude that any contact point \mathbf{p} on an object shape S can in fact be parameterized minimally by two variables, h and θ . In this work, we show that analyzing the task constraints, robot limitations and contact models in this low-dimensional subspace leads to significant efficiency gains in grasp planning.

3.1.1 Mapping Euclidean Coordinates to a Cylindrical Coordinate System

To reason about tasks traditionally expressed in Euclidean coordinates, we introduce a mapping between the representation of a point in the Euclidean world frame, p_w , to the $\mathbf{x} = [h, \theta]^T$ parameters in the a cylindrical coordinate system \mathbb{S} . First, we define the local object frame L in the Euclidean coordinate frames by using the principal axis (i.e. axis of symmetry) \mathbf{z} , the polar axis \mathbf{a} , and their cross-product. Given the pose of an object in the world coordinates, T_l^w , we can first transform the point into the local object space, $p^l = T_l^w p^w$, and then map it to the surface representation \mathbf{x} using the function $f: \mathbb{R}^3 \rightarrow \mathbb{S}$:

$$f(\mathbf{p}^l) = f([x, y, z]^T) = \begin{bmatrix} z \\ \text{atan2}(y, x) \end{bmatrix}. \quad (1)$$

Once a planner reasons about the environment and a contact point is determined in the cylindrical surface representation, we need to map it back to the Euclidean space using an inverse mapping $f^{-1}: \mathbb{S} \rightarrow \mathbb{R}^3$:

$$f^{-1}(\mathbf{x}) = f^{-1}([h, \theta]^T) = \begin{bmatrix} r(h) \cos(\theta) \\ r(h) \sin(\theta) \\ h \end{bmatrix}. \quad (2)$$

Fig. 3 depicts the forward mapping process moving from the local object frame to the cylindrical surface representation. Observe that the surface of the example soda can be unwrapped into a smooth finite two-dimensional plane with minimal distortion because the object is rotationally symmetric, and does not have protrusions nor cavities.

3.2 Grasp Manifold

Stable grasps can be rotated around the principle axis of rotationally symmetric objects without having to modify the hand shape. Moreover, the relative rotation between a predefined grasp and an object can be captured with a simple linear motion model in the reduced 2D cylindrical manifold. To demonstrate the advantages of this key idea, we begin

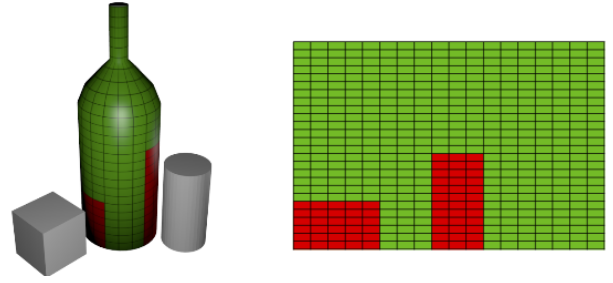


Figure 4: For each cell of the wine bottle we check for collisions and reachability and store the result in a map representing the corresponding low-dimensional manifold. Red cells are grasp locations that would lead to collisions or are unreachable.

our analysis with a simplified manipulation model where a point on the object surface corresponds to a wrist position during grasping. Moreover, the hand is assumed to be parallel to the base of the object such that the plane between the grasping fingers is perpendicular to the axis of symmetry.

Given a predefined hand shape and a task definition, the planner needs to choose a contact point, $\mathbf{x} = [h, \theta]$, that represents its wrist position. Feasible contact points are characterized by collision-free inverse kinematic solutions where at least one manipulator pose should exist that both reaches the desired point and does not collide with the environment. Fig. 4 visualizes this concept. We can discretize the manifold representation using a regular grid. Each cell can then be mapped to the bottle object. For each cell of the discretized manifold, using the center point as the reference for the wrist, we attempt to compute a collision-free inverse kinematics solution. In Fig. 4, red cells indicate collisions, while green cells indicate collision-free grasp locations.

In addition to the physical feasibility of a contact point, its functionality towards accomplishing tasks also needs to be taken into account in grasp selection. For instance, if an object is picked with the purpose of placing it down in another cluttered environment, collisions in the second scene also need to be accounted for. Similarly, a task may require an object to be configured at a specific pose, i.e. pouring water from a bottle to a cup, in which case the planner should account for the reachability of that pose with the *foresight* that the same grasp would have to be utilized.

3.2.1 Modeling Task Constraints in Cylindrical Space

Most everyday grasps require reasoning about multiple tasks even though the tasks may take place in substantially different environments with varying constraints on the pose of the manipulated object. Although the locations and requirements of the tasks may vary, they all impose constraints on the same gripper-object system since once an object is picked, the grasp cannot be changed. We exploit the *invariance* of the gripper-object relationship in manipulation tasks with rotationally symmetric objects, where the task descriptions naturally account for all the degrees of freedom but the rotation around axis of symmetry since the rotation does not effect object properties. The goal is to autonomously exploit the under-constrained task specifications by planning for object rotations and grasp positions. By only modelling grasps that are perpendicular to the axis

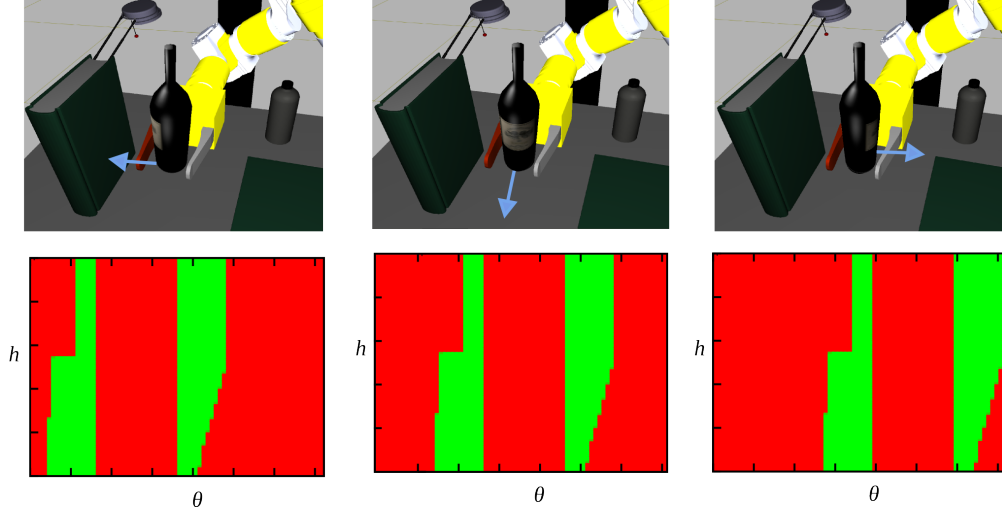


Figure 5: Visualization of the task constraints with a rotating bottle. We can see that the entries of the low-dimensional manifold only shift when the object rotates around its axis of symmetry. This feature is a key insight of this paper. It follows, that there is a simple update procedure for the entries.

of symmetry, e.g. grasp rotates around object, we induce a coupling between gripper and object poses. Now, *given a single pair of gripper and object poses that is known to satisfy task constraints, an infinite number of new pairs can be generated by rotating the gripper around the object by some θ degrees and rotating the object around itself by $-\theta$.* Moreover, by determining the feasible set of contacts for an initial object pose which satisfies task requirements, we can extrapolate to a family of object rotations and corresponding contact placements. This extrapolation is only feasible because the rotation of the object around its axis and the rotation of the grasp around the object are coupled by the θ variable around the principle axis \mathbf{z} and thus, we reason about task constraints in the cylindrical parameter space.

A crucial property of this representation is that the produced map can be efficiently updated when the object is rotated around its axis of symmetry. More specifically, a rotation around the z -axis corresponds to a shift along the θ dimension.

3.2.2 Extrapolating Task Constraints to new Object Rotations

The analysis of grasp feasibility for a given object pose and task description can be utilized to reason about grasp selection if the object is rotated only around its axis of symmetry. The idea is that the coupling between the rotation of the grasp around the object pose and the rotation of the object around its own principle axis can be utilized to generate previously examined grasps for new object rotations and to adopt the successful examples. The invariance of task constraint effects on gripper-object systems to interactions between the gripper and the object poses that do not change gripper configuration in the task space can be analyzed formally.

Let the function $m : \mathbb{S}, SE(3) \rightarrow \{0, 1\}$ represent a mapping from a 6-DOF object pose $T^w \in SE(3)$ and a contact pose on the object surface, $\mathbf{x} = [h, \theta]^T \in \mathbb{S}$, to a binary evaluation of whether a grasp is feasible. The feasibility of

a grasp may depend on a variety of criteria such as inverse kinematics, collisions, torque limits, manipulability and etc. In this work, we focus on collision-free inverse kinematics and define the operator $ik : SO(3), \mathbb{R}^3 \rightarrow \{0, 1\}$ that evaluates whether an arm configuration exists that can achieve the end-effector rotation $R_e^w \in SO(3)$ and location $t_e^w \in \mathbb{R}^3$.

We claim that given the mapping of feasibility grasps for an initial object pose T_o^w , the feasibility of any grasp $x \in \mathbb{S}$, for a new pose T_{o2}^w , can be deduced by using the previous mapping:

$$m([h, \theta], T_{o2}^w) = m([h, \theta + \delta], T_o^w) \quad (3)$$

where $T_{o2}^w = T_o^w R^z(\delta)$ where $R^z(\delta)$ is a rotation matrix around the local z -axis by angle δ (the notation $T^z(\delta)$ also represents a transformation matrix with the rotation $R^z(\delta)$ but no translation). The claim is proven by showing that the gripper and object rotations counteract each other:

$$\begin{aligned} m([h, \theta]^T, T_{o2}^w) &= \\ &= ik(R_{o2}^w R^z(\theta), T_{o2}^w f^{-1}([h, \theta]^T)) \end{aligned} \quad (4)$$

$$= ik(R_o^w R^z(\delta) R^z(\theta), T_o^w T^z(-\delta) f^{-1}([h, \theta + \delta]^T)) \quad (5)$$

$$= ik(R_o^w R^z(\theta + \delta), T_o^w f^{-1}([h, \theta + \delta]^T)) \quad (6)$$

$$= m([h, \theta + \delta]^T, T_o^w). \quad (7)$$

The proof starts by reducing the mapping to the inverse kinematics problem where the wrist orientation is computed in the world coordinate frame by composing the second object rotation R_{o2}^w with the contact angle offset θ . Similarly, the end-effector position is computed by composing the second object transform T_{o2}^w with the contact position in the local coordinates obtained with inverse cylindrical mapping $T^{o2} = f^{-1}([h, \theta]^T)$. The key insight takes place in Equation 5 where the cylindrical object representation is rotated by δ degrees all the while the pose of the object is rotated in the opposite direction by composing with $T^z(-\delta)$. Equations 6 and 7 simply reorganize the terms to show that the

initial feasibility mapping can be reduced from the inverse kinematics formulation.

Fig. 5 depicts the main insight which is discussed in this section. As an object rotates around its axis of symmetry, the entries in the low-dimensional map shift according to the δ angle. Hence, adding to all entries is enough to update the map whenever the object rotates around its axis of symmetry. Subsequently we will refer to the map holding information about feasibility in the low-dimensional space as a *feasibility map*.

4. GRASP PLANNING WITH GRASP MANIFOLDS

We can exploit the introduced concepts for robot grasp planning with foresight. The idea is to calculate for each subtask of the complex task a corresponding feasibility map. Feasibility maps can, then, be collectively analyzed in order to identify a grasp that is fulfills the constraints of current and future actions.

The first step in grasp planning is to generate the feasibility map for each sub-task. Algorithm 1 shows how a binary 2D feasibility map can be generated. The idea is to discretize the low-dimensional manifold, map the center of each cell back into the high-dimensional space and then check for collisions and reachability.

Algorithm 1: CreateMap(): Generates feasibility maps

Input: $\{\hat{h}, \check{h}, \hat{\theta}, \check{\theta}\}$: min/max height and angle limits, $\{\delta h, \delta \theta\}$: increments, R : robot, W : world

Result: M : Binary 2D array with feasibility indicators

```

1 for  $h \leftarrow \hat{h}$  to  $\check{h}$  do
2   for  $\theta \leftarrow \hat{\theta}$  to  $\check{\theta}$  do
3      $p^l \leftarrow [r \cos(\theta), r \sin(\theta), h]^T$ ; // Inverse mapping
4      $p^w \leftarrow W.objectPose() * p^l$ ; // Goal wrist pose
5     for  $\phi \leftarrow 0$  to  $2\pi$  do // Sample redundancy
6        $R.analyticalIK(W.objectPose(), p^w, \phi)$ ;
7       if  $W.collisionFree()$  then
8          $M[(h - \hat{h})/\delta h][(\theta - \hat{\theta})/\delta \theta] \leftarrow 1$ ;
9         jump to line 2;
10     $\theta \leftarrow \theta + \delta \theta$ ;
11   $h \leftarrow h + \delta h$ ;
12 return  $M$ ;
```

4.1 Planning for Task Sequences

Given the feasibility maps for each subtask in a sequence of tasks, we can generate an appropriate grasp by reasoning about the intersections of grasp projections onto the object space. Algorithm 2 uses the precomputed projections of task constraints on the object spaces to reason about how to rotate the objects in the poses constrained by the tasks.

Figure 6 demonstrates the shifting of feasibility maps over each other to find proper grasps that satisfy all the tasks.

4.2 Reasoning about Handprints for Bimanual Tasks

Figure 7 demonstrates the projection of handprints onto the surface manifold where two hands drawn with blue and

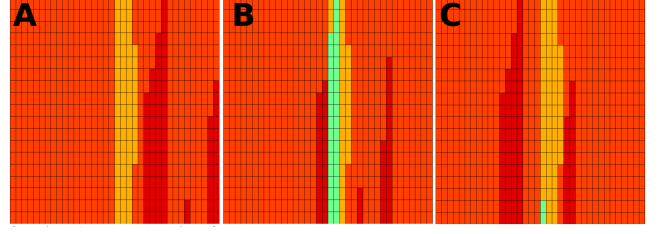


Figure 6: Two superimposition of two maps on top of each other as one of the objects move

Algorithm 2: Single Grasp for Sequential Tasks

Input: $\{\hat{h}, \check{h}, \hat{\theta}, \check{\theta}\}$: min/max height and angle limits, $\{\delta h, \delta \theta\}$: increments, R : robot, W : world, T : object poses for tasks

Result: $\{h, \theta\}$: grasp pose, δ_i : task rotations

```

1 for  $T \in \mathbb{T}$ ,  $i \leftarrow 0$  do // Generate maps for each task
2    $W.setObjectPose(T)$ ;
3    $M[i] = \text{CreateMap}(\hat{h}, \check{h}, \hat{\theta}, \check{\theta}, R, W)$ ;
4    $i \leftarrow i + 1$ ;
5 for  $h \leftarrow \hat{h}$  to  $\check{h}$  do // Iterate through object height
6    $\theta^* \leftarrow -1$ ;
7   for  $\theta \leftarrow \hat{\theta}$  to  $\check{\theta}$  do // Find grasp pose on 1st object
8     if  $M[(h - \hat{h})/\delta h][(\theta - \hat{\theta})/\delta \theta] = 1$  then
9        $\theta^* \leftarrow \theta$ ;
10      break;
11     $\theta \leftarrow \theta + \delta \theta$ ;
12  if  $\theta^* = -1$  then continue;
13  foundAll  $\leftarrow$  true;
14  for  $T \in \mathbb{T}$ ,  $i \leftarrow 0$  do // Find grasps for each task
15    for  $\theta \leftarrow \hat{\theta}$  to  $\check{\theta}$  do
16      if  $M[(h - \hat{h})/\delta h][(\theta - \hat{\theta})/\delta \theta] = 1$  then
17         $\delta_i \leftarrow \theta - \theta^*$ ;
18        break;
19       $\theta \leftarrow \theta + \delta \theta$ ;
20    if  $\delta_i = \emptyset$  then
21      foundAll  $\leftarrow$  false;
22      break;
23  if foundAll then return  $\{h, \theta^*, \delta_i \forall i\}$ ;
24   $h \leftarrow h + \delta h$ ;
25 return  $\emptyset$ ;
```

yellow profiles can be seen colliding with each other. The algorithm 3 uses a hill-climbing approach to minimize the intersection of handprints to move the hands further away from each other as can be seen on the right hand side of Figure 7. The computation of the hand positions were in average 23 milliseconds especially when there was a large space of feasible grasps.

5. DISCUSSION

The presented planner can be seen as a first prototype of grasp planning algorithms that exploit symmetry and other shape properties. The main contribution is a low-

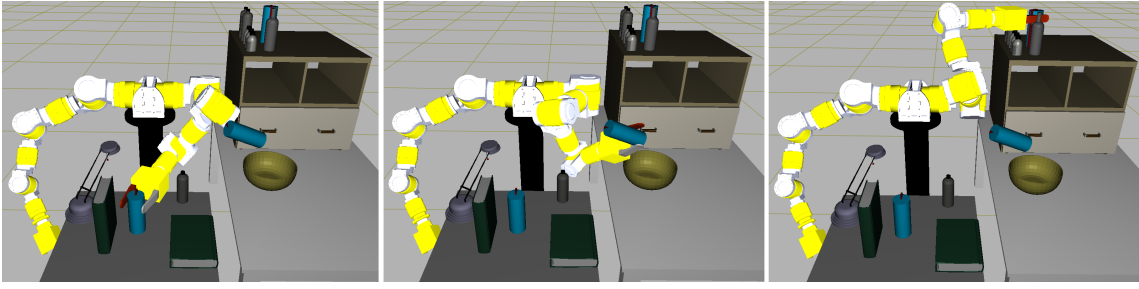


Figure 8: Computation of a single grasp across multiple tasks where the robot has to pick up a bottle, pour its contents into a bowl and place it down.

Algorithm 3: Collaborative Grasps on Single Task

Input: $\{\hat{h}, \check{h}, \hat{\theta}, \check{\theta}\}$: min/max height and angle limits,
 $\{\delta h, \delta \theta\}$: increments, \mathbb{R} : robots, W : world,
 \mathbb{H} : hand prints

Result: $\{h_i, \theta_i\}$: grasp poses for each robot

```

1 for  $R \in \mathbb{R}$ ,  $i \leftarrow 0$  do // Generate maps for each robot
2    $M[i] = \text{CreateMap}(\hat{h}, \check{h}, \hat{\theta}, \check{\theta}, R, W)$ ;
3    $i \leftarrow i + 1$ ;
4 for  $\text{restart} \leftarrow 0$  to  $\text{MAX\_RESTARTS}$  do
5   for robot  $R \in \mathbb{R}$ ,  $i \leftarrow 0$  do // Sample contacts
6      $[h_i, \theta_i] \leftarrow \text{random}(\hat{h}, \check{h}, \hat{\theta}, \check{\theta}, \delta h, \delta \theta)$ ;
7      $i \leftarrow i + 1$ ;
    // Minimize collisions by moving random grasp
8   for  $\text{iters} \leftarrow 0$  to  $\text{MAX\_ITERS}$  do
9     // Stop if all the grasps are collision free
10    if  $W.\text{collisionFree}()$  then return  $\{h_i, \theta_i\}$ ;
11     $R \leftarrow \mathbb{R}[\text{random}()]$ ; // Choose random robot
12     $\text{dirs} \leftarrow \{\{\delta h, 0\}, \{0, \delta \theta\}, \{-\delta h, 0\}, \{0, -\delta \theta\}\}$ ;
13     $\text{minNumColls} \leftarrow \infty$ ,  $\text{bestDir} \leftarrow \emptyset$ ;
14    for  $\text{dir} \in \text{dirs}$  do
15       $h^* \leftarrow h_R + \text{dir}[0]$ ,  $\theta^* \leftarrow \theta_R + \text{dir}[1]$ ;
16      if  $M[(h^* - \hat{h})/\delta h][(\theta^* - \hat{\theta})/\delta \theta] = 0$ ; then
17        continue;
18       $\text{numColls} \leftarrow \text{countCollisions}(W)$ ;
19      if  $\text{numColls} < \text{minNumColls}$  then
20         $\text{minNumColls} \leftarrow \text{numColls}$ ;
21         $\text{bestDir} \leftarrow \text{dir}$ ;
    // Update grasp with minimum collision direction
22     $h^* \leftarrow h_R + \text{bestDir}[0]$ ,  $\theta^* \leftarrow \theta_R + \text{bestDir}[1]$ ;
23     $h_r \leftarrow h^*$ ,  $\theta_r \leftarrow \theta^*$ ;
24 return  $\emptyset$ ;
```

dimensional representation that allows us to store and analyze information about grasp feasibility for sequential or parallel grasping actions. While we showed that this can be used for efficient planning, there are various aspects of our approach that need further investigation. At the moment we assume a discretization of the manifold. It is unclear how this discretization affects the robot performance and how the discretization parameters need to be chosen. So far, we have shown that grasps can be rotated around the axis of symmetry without modification. However, if the hand is moving

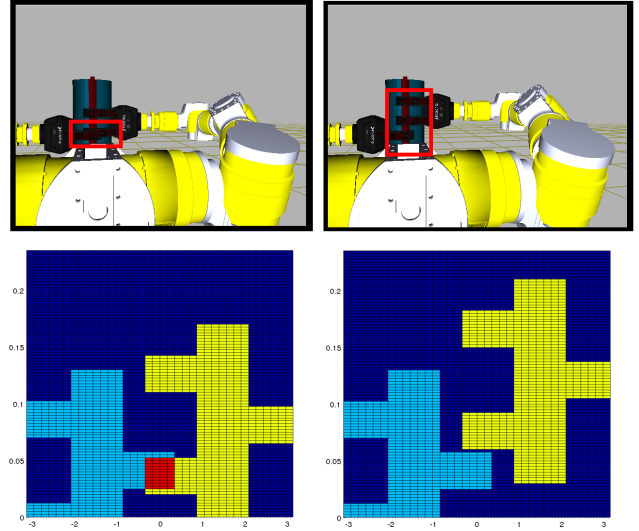


Figure 7: The projection of hand prints onto the object surface and the detection of finger collisions

up and down along the axis of symmetry, the hand shape might have to be changed. This is particularly true in cases where the object radius drastically changes, i.e. very curvy objects. In such cases, the hand shape needs to be adapted to the new radius. We believe that, similar to the HSV color space in computer vision, we can create a 3D space which augments the current manifold with another dimension for the radius at different heights. This would allow us to model hand shape variations along the axis of symmetry. So far, our study has shown that object-centered representations can be very powerful representations for grasp planning. However, we believe that more interesting properties and insights about such representations can possibly be identified. The key to grasp planning with foresight, is to use prior knowledge about re-occurring and natural shape properties, e.g. symmetries and extrusions, to generate low-dimensional grasp representations.

6. CONCLUSION

In this paper we presented a grasp planning algorithm that exploits rotational symmetries for generating task-constrained grasps. One of the major results is presented in Figure 8

where a sequence of tasks have been considered to compute a single grasp that satisfies all of their constraints. The algorithm is particularly suited for grasp planning with several subtasks or several interacting agents. The key insight of the paper is that re-occurring patterns in the geometry of shapes can be exploited to drastically reduce the space of solutions. To this end, we introduced a low-dimensional, object-centered representation for grasp planning which is based on rotational symmetries. Since such objects are symmetric, any stable grasp can be rotated around the axis yielding a family of feasible grasps. We presented early results showing that this property allows us to generate multiple grasps around an object, which is useful for bi-manual tasks and cooperative robot hand over tasks.

REFERENCES

- [1] L. Antanas, P. Moreno, M. Neumann, R. Pimentel de Figueiredo, K. Kersting, J. Santos-Victor, and L. De Raedt. High-level Reasoning and Low-level Learning for Grasping: A Probabilistic Logic Pipeline. *ArXiv e-prints*, November 2014.
- [2] H. Ben Amor, O. Kroemer, U. Hillenbrand, G. Neumann, and J. Peters. Generalization of human grasping for multi-fingered robot hands. In *Intelligent Robots and Systems (IROS), 2012 IEEE/RSJ International Conference on*, pages 2043–2050, Oct 2012.
- [3] Jeannette Bohg, Matthew Johnson-Roberson, Beatriz León, Javier Felip, Xavi Gratal, N Bergstrom, Danica Kragic, and Antonio Morales. Mind the gap-robotic grasping under incomplete observation. In *Robotics and Automation (ICRA), 2011 IEEE International Conference on*, pages 686–693. IEEE, 2011.
- [4] C. Borst, M. Fischer, and G. Hirzinger. Grasp planning: how to choose a suitable task wrench space. In *Robotics and Automation, 2004. Proceedings. ICRA '04. 2004 IEEE International Conference on*, volume 1, pages 319–325 Vol.1, April 2004.
- [5] Matei T. Ciocarlie and Peter K. Allen. Hand posture subspaces for dexterous robotic grasping. *Int. J. Rob. Res.*, 28(7):851–867, July 2009.
- [6] Hao Dang and Peter K. Allen. Semantic grasping: planning task-specific stable robotic grasps. *Autonomous Robots*, 37(3):301–316, 2014.
- [7] Corey Goldfeder, Peter K Allen, Claire Lackner, and Raphael Pelossof. Grasp planning via decomposition trees. In *Robotics and Automation, 2007 IEEE International Conference on*, pages 4679–4684. IEEE, 2007.
- [8] Kai Huebner and Danica Kragic. Selection of robot pre-grasps using box-based shape approximation. In *Intelligent Robots and Systems, 2008. IROS 2008. IEEE/RSJ International Conference on*, pages 1765–1770. IEEE, 2008.
- [9] T. Asfour J. Bohg, A. Morales and D. Kragic. Data-driven grasp synthesis – a survey. *IEEE Transactions on Robotics*, 30(2):289–309, 2014.
- [10] U. Klank, D. Pangercic, R.B. Rusu, and M. Beetz. Real-time cad model matching for mobile manipulation and grasping. In *Humanoid Robots, 2009. Humanoids 2009. 9th IEEE-RAS International Conference on*, pages 290–296, Dec 2009.
- [11] D. Kragic, AT. Miller, and P.K. Allen. Real-time tracking meets online grasp planning. In *Robotics and Automation, 2001. Proceedings 2001 ICRA. IEEE International Conference on*, volume 3, pages 2460–2465 vol.3, 2001.
- [12] O. Kroemer, H. Ben Amor, M. Ewerton, and J. Peters. Point cloud completion using extrusions. In *Proceedings of the International Conference on Humanoid Robots (HUMANOIDS)*, 2012.
- [13] Martin Levihn, Leslie Pack Kaelbling, Tomás Lozano-Pérez, and Mike Stilman. Foresight and reconsideration in hierarchical planning and execution. In *IEEE/RSJ International Conference on Intelligent Robots and Systems*, 2013.
- [14] Andrew T Miller, Steffen Knoop, Henrik I Christensen, and Peter K Allen. Automatic grasp planning using shape primitives. In *Robotics and Automation, 2003. Proceedings. ICRA '03. IEEE International Conference on*, volume 2, pages 1824–1829. IEEE, 2003.
- [15] V.-D. Nguyen. Constructing force-closure grasps. In *Robotics and Automation. Proceedings. 1986 IEEE International Conference on*, volume 3, pages 1368–1373, Apr 1986.
- [16] Markus Przybylski, Tamim Asfour, and Rüdiger Dillmann. Unions of balls for shape approximation in robot grasping. In *Intelligent Robots and Systems (IROS), 2010 IEEE/RSJ International Conference on*, pages 1592–1599. IEEE, 2010.
- [17] A. Sahbani, S. El-Khoury, and P. Bidaud. An overview of 3d object grasp synthesis algorithms. *Robot. Auton. Syst.*, 60(3):326–336, March 2012.
- [18] D. Song, K. Huebner, V. Kyrki, and D. Kragic. Learning task constraints for robot grasping using graphical models. In *Intelligent Robots and Systems (IROS), 2010 IEEE/RSJ International Conference on*, pages 1579–1585, Oct 2010.
- [19] Nikolaus Vahrenkamp, Tamim Asfour, and Rüdiger Dillmann. Simultaneous grasp and motion planning. *IEEE Robotics and Automation Magazine - Special Issue on Mobile Manipulation*, pages 43–57, 2012.